Electrical activity-triggered glucagon-like peptide-1 secretion from primary murine L-cells

G. J. Rogers, G. Tolhurst, A. Ramzan, A. M. Habib, H. E. Parker, F. M. Gribble and F. Reimann

Cambridge Institute for Medical Research, Wellcome Trust/MRC Building, Addenbrooke's Hospital, Box 139, Hills Road, Cambridge CB2 0XY, UK

Non-technical summary Glucagon like peptide 1 (GLP-1) based therapies are now widely used for the treatment of diabetes. The physiological source of the hormone is the intestinal L-cell, and attempts to boost secretion have been hindered by difficulties in distinguishing these cells from their epithelial neighbours and our consequent limited understanding of their physiology. Using recently developed transgenic mice with fluorescently labelled L-cells, we show that these cells are electrically active and use voltage-gated ion channels to couple the presence of nutrients to the secretion of GLP-1. We present the identification and characterisation of the ion channels. This improves our understanding of enteroendocrine physiology and will support therapeutic programmes aiming to target gut hormone secretion.

Abstract Glucagon like peptide 1 (GLP-1) based therapies are now widely used for the treatment of type 2 diabetes. Developing our understanding of intestinal GLP-1 release may facilitate the development of new therapeutics aimed at targeting the GLP-1 producing L-cells. This study was undertaken to characterise the electrical activity of primary L-cells and the importance of voltage gated sodium and calcium channels for GLP-1 secretion. Primary murine L-cells were identified and purified using transgenic mice expressing a fluorescent protein driven by the proglucagon promoter. Fluorescent L-cells were identified within primary colonic cultures for patch clamp recordings. GLP-1 secretion was measured from primary colonic cultures. L-cells purified by flow cytometry were used to measure gene expression by microarray and quantitative RT-PCR. Electrical activity in L-cells was due to large voltage gated sodium currents, inhibition of which by tetrodotoxin reduced both basal and glutamine-stimulated GLP-1 secretion. Voltage gated calcium channels were predominantly of the L-type, Q-type and T-type, by expression analysis, consistent with the finding that GLP-1 release was blocked both by nifedipine and ω-conotoxin MVIIC. We observed large voltage-dependent potassium currents, but only a small chromanol sensitive current that might be attributable to KCNQ1. GLP-1 release from primary L-cells is linked to electrical activity and activation of L-type and Q-type calcium currents. The concept of an electrically excitable L-cell provides a basis for understanding how GLP-1 release may be modulated by nutrient, hormonal and pharmaceutical stimuli.

F. M. Gribble and F. Reimann contributed equally to the work.

Introduction

Glucagon like peptide-1 is an insulinotropic hormone released from intestinal L-cells in response to food ingestion. In view of the recent success of GLP-1 mimetics and inhibitors of GLP-1 degradation for the treatment of type 2 diabetes (Drucker & Nauck, 2006), attention is turning towards whether it would be feasible and beneficial to target the L-cells, thereby enhancing the endogenous release of GLP-1, together with the other anorectic peptides, peptide YY (PYY) and oxyntomodulin (Holst, 2007; Gribble, 2008). Understanding the sensory and secretory pathways in L-cells is key to the success of this strategy.

L-cells are open-type enteroendocrine cells, with apical processes facing the gut lumen (Eissele *et al.* 1992) that are believed to play a role in nutrient sensing. They are responsive to a range of luminal components, particularly the digestion products of carbohydrates, fats and protein (Elliott *et al.* 1993; Herrmann *et al.* 1995). The nature of their sensory apparatus remains poorly understood, although studies in the GLP-1 secreting cell line GLUTag (Drucker *et al.* 1994) suggested that electrogenic uptake of glucose or amino acids triggers membrane depolarisation, electrical activity and Ca^{2+} entry through L- and N-type voltage gated Ca^{2+} channels (Gribble *et al.* 2003, 2008; Reimann *et al.* 2004, 2005).

The finding that GLUTag cells fired action potentials carried by voltage gated Na^+ channels (Reimann *et al.* 2005) was slightly surprising, in the light of the reported electrophysiological properties of other types of enteroendocrine cell. Actually, there have been very few electrophysiological studies of primary enteroendocrine cells, because these cells comprise only a small sub-population of the intestinal epithelium and are difficult to isolate, purify and identify. One population that has received attention, as they are more easily distinguishable from their neighbours, is the enterochromaffin like (ECL) cell, responsible for histamine secretion in the stomach. ECL cells differ from L-cells in being closed-type, i.e. they do not make direct connection with the gut lumen, and are activated primarily by hormonal and neuronal vagal signals. Unlike the findings from GLUTag cells, electrophysiological studies of single isolated ECL cells have concluded that they do not possess V-gated Na^+ currents and are therefore unlikely to be electrically active (Prinz *et al.* 2003).

To enable studies on primary GLP-secreting cells, we recently generated transgenic mice in which the proglucagon promoter drives expression of a yellow fluorescent protein derivative, Venus (Reimann *et al.* 2008). L-cells in GLU-Venus mice are brightly fluorescent and can be purified by flow cytometry, or identified and monitored in mixed primary cultures of colonic epithelium from adult mice. Like GLUTag cells,

we reported that primary L-cells employ sodium coupled glucose transporters (SGLT1) as their primary glucose-sensing machinery, and that this is likely to be coupled to GLP-1 secretion through membrane depolarisation, electrical activity and Ca^{2+} entry (Reimann *et al.* 2008). To understand better the link between depolarisation and GLP-1 release, the current study was set up to establish the properties and molecular identity of the currents underlying electrical activity and the Ca^{2+} influx pathways in primary L-cells.

Methods

Intestinal epithelial cell isolation

Animal procedures were approved by the local ethical committee, conforming to UK Home Office regulations and following the Principles of Laboratory Care. Two- to six-month-old GLU-Venus C57B6 transgenic mice were killed by cervical dislocation and the gut collected into ice-cold Leibovitz-15 medium (PAA Laboratories Ltd, Yeovil, UK). For culture, tissue was digested 3 times in collagenase XI ($0.4\ mg\ ml^{-1}$) in Dulbecco's modified Eagle's medium (DMEM, $25\ mmol\ l^{-1}$ glucose) for 10–15 min at $37°C$. Supernatants were centrifuged at $300\ g$ and the pellets re-suspended in DMEM supplemented with 10% FBS, $2\ mmol\ l^{-1}$ L-glutamine, $100\ units\ ml^{-1}$ penicillin and $0.1\ mg\ ml^{-1}$ streptomycin. Aliquots were plated on Matrigel-coated (BD Biosciences, Oxford, UK) 24-well plates or 35 mm plastic dishes for secretion and electrophysiology studies, respectively, and incubated for 1–14 days at $37°C$, 5% CO_2.

Flow cytometry

Venus positive cells were purified from GLU-Venus colonic tissue, digested to single cells with $1\ mg\ ml^{-1}$ collagenase in Hanks' buffered salt solution. Cell suspensions were separated by flow cytometry to obtain populations of >95% pure Venus positive or negative (control) cells, as described previously (Reimann *et al.* 2008). Cells were sorted at numbers of up to 30,000 into lysis buffer for mRNA extraction.

RNA extraction and quantitative RT-PCR

Total RNA from fluorescence-activated cell sorting (FACS) and GLUTag cells was isolated using a micro scale RNA isolation kit (Applied Biosystems, Warrington, UK) and a TRI Reagent protocol, respectively. Both were reverse-transcribed according to standard protocols. Quantitative RT-PCR was performed with 7900 HT Fast Real-Time PCR system (Applied Biosystems), using primers/probes (Applied

Biosystems) for *scn3a* (Mm00658167_m1), *scn5a* (Mm00451971_m1), *scn11a* (Mm00449377_m1), *cacna1a* (Mm00432190_m1), *cacna1b* (Mm01333678_m1), *cacna1c* (Mm00437917_m1), *cacna1d* (Mm01209919_m1), *cacna1h* (Mm00445369_m1), *kcnq1* (Mm00434641_m1) and *kcne3* (Mm00445119_m1). The PCR reaction mix consisted of first-strand cDNA template, primer pairs, 6-carboxyfluorescein/quencher probes, and PCR Master mix (Applied Biosystems). Expression was compared with that of β-*actin* measured on the same sample, giving a C_T difference (ΔC_T) for β-*actin* minus the test gene. Mean, standard error of the mean and statistics were performed on the ΔC_T data, and converted to relative expression levels ($2^{\Delta C_T}$) for presentation in the figures.

Microarray analysis

RNA intended for gene expression profiling was extracted from L-cells FACS-purified from three to four animals per run. This underwent two rounds of *in vitro* amplification (MessageAmp mRNA amplification kit, Applied Biosystems), during which target RNA was labelled with biotin-16-UTP (Enzo Life Sciences UK Ltd, Exeter, UK). RNA was hybridised against Affymetrix mouse 430 2.0 expression arrays (Affymetrix UK Ltd, High Wycombe, UK). Expression levels of each probe were determined by robust multichip average (RMA) analysis. Our experience is that RMA values >100 represent expression levels that can be robustly verified by quantitative RT-PCR.

Hormone secretion

Secretion studies were performed 1–5 days after plating using tissue from either transgenic or non-transgenic mice (Reimann *et al.* 2008). Cultures were incubated with test reagents in bath solution (see below) containing 0.1% fatty acid-free BSA for 2 h at 37°C. For experiments involving different K^+ concentrations, standard bath solution was mixed at an appropriate ratio with a modified bath solution in which Na^+ was replaced by K^+. Supernatants were collected and centrifuged to remove contaminating cells. The remaining adherent cells were treated with lysis buffer containing: 50 mmol l^{-1} Tris-HCl, 150 mmol l^{-1} NaCl, 1% IGEPAL-CA 630, 0.5% deoxycholic acid and one tablet of complete EDTA-free protease inhibitor cocktail (Roche), to extract intracellular peptides. GLP-1 was assayed in supernatants and cell extracts using an active GLP-1 ELISA-kit (Millipore UK Ltd, Watford, UK), Hormone secretion was expressed as a fraction of the total hormone content of each well, and normalised, as indicated, to the basal secretion measured in parallel on the same day.

Electrophysiology

Experiments were performed on identified Venus positive cells in 5- to 14-day-old colonic cultures of GLU-Venus mice. Microelectrodes were pulled from borosilicate glass (GC150 T, Harvard Apparatus, Edenbridge, UK) and the tips coated with refined yellow beeswax. Electrodes were fire-polished using a microforge (Narishige, London, UK) and had resistances of 2.5–3 MΩ when filled with pipette solution. Membrane potential and currents were recorded using a HEKA EPC10 amplifier and Patchmaster/Pulse software (Digitimer Welwyn Garden City, UK) or an Axopatch 200B and pCLAMP software (Molecular Devices, Wokingham, UK). Electrophysiological recordings were made using either the standard whole cell or perforated patch configuration of the patch clamp setup, at 22–24°C. Standard whole cell currents were zero and leak subtracted using HEKA Pulsefit or Patchmaster software and a *P*/4 protocol.

Solutions and chemicals

The standard bath solution contained (mmol l^{-1}): 4.5 KCl, 138 NaCl, 4.2 NaHCO$_3$, 1.2 NaH$_2$PO$_4$, 2.6 CaCl$_2$, 1.2 MgCl$_2$, and 10 Hepes (pH 7.4, NaOH). For Na$^+$ currents, K$^+$ was replaced with Cs$^+$, 10 mmol l^{-1} 4-aminopyridine (4-AP) was added to the bath solution and Na$^+$ was partially replaced by 20 mmol l^{-1} tetraethylammonium (TEA$^+$). The same solution was used to record Ca^{2+} currents after the addition of 0.3 μmol l^{-1} tetrodotoxin (TTX). When Ba^{2+} was used as the charge carrier, HCO$_3^-$ and H$_2$PO$_4^-$ were additionally replaced with Cl$^-$. To record K$^+$ currents, TTX (0.3 μmol l^{-1}) was added to the standard bath solution and Na$^+$ was partially replaced with TEA$^+$ (20 mmol l^{-1}), where indicated. Electrophysiological recordings were performed in the presence of 1 mmol l^{-1} glucose unless otherwise stated. The perforated patch pipette solution contained (mmol l^{-1}): 76 K$_2$SO$_4$, 10 KCl, 10 NaCl, 55 sucrose, 10 Hepes, 1 MgCl$_2$, (pH 7.2), plus amphotericin B at 200 μg ml^{-1}. The standard whole cell patch pipette solution contained (mmol l^{-1}): 107 KCl, 1 CaCl$_2$, 7 MgCl$_2$, 11 EGTA, 10 Hepes, 5 K$_2$ATP (pH 7.2 with KOH). For Na$^+$ and Ca^{2+} current recordings K$^+$ was replaced by Cs$^+$ and Na$_2$ATP was used. Drugs and chemicals were purchased from Sigma-Aldrich (Poole, UK) unless otherwise stated. ω-Conotoxin GVIA and ω-Conotoxin MVIIC were purchased from Alomone Labs (Jerusalem, Israel) and Peptide Institute, Inc. (Osaka, Japan). ω-Agatoxin IVA was purchased from Alomone Labs and tetrodotoxin was from Tocris Bioscience (Bristol, UK). CsCl and CsOH were from Alfa Aesar (Heysham, UK).

Data analysis

Data were analysed with Origin software (Aston Scientific, Milton Keynes, UK), using the following equations.
Equation 1 (for voltage-dependent Na$^+$ current activation):

$$I = (A + (g_{max} - A)/(1 + e^{((V_h - V_m)/k)})) \times (V_m - V_{rev})$$

where g is the conductance, g_{max} is the maximum conductance, V_m is the membrane potential, V_h is the voltage at which channels are half activated, and k is a constant.
Equation 2 (for voltage dependent inactivation):

$$g/g_{max} = 1/(1 + e^{((V_m - V_h)/k)})$$

Equation 3 (for voltage dependent activation of K$^+$ channels)

$$I = g_{max} \times (V_m + 80)/(1 + e^{((V_h - V_m)/k)})$$

Equation 4 (for voltage dependent activation of two Ca^{2+} current populations)

$$I = (A + (g_{max\,1} - A)/(1 + e^{((V_{h1} - V_m)/k_1)})) \times (V_m - V_{rev})$$
$$+ (A + (g_{max\,2} - A)/(1 + e^{((V_{h2} - V_m)/k_2)})) \times (V_m - V_{rev})$$

Where g_{max1}, V_{h1} and k_1 represent the parameters of a first Ca^{2+} channel population, and g_{max2}, V_{h2} and k_2 represent the second population.

Statistical comparisons were performed by Student's *t* test or regression analysis, as indicated, using Microsoft Excel. The threshold for assigning significance was $P < 0.05$. Data are presented as means and standard errors of the mean.

Results

Primary colonic L-cells in perforated patch recordings are electrically active, with a threshold for action potential initiation of -36 ± 1 mV ($n = 17$; Fig. 1A). Action potentials were observed to overshoot to a mean positive membrane potential of $+48 \pm 8$ mV ($n = 17$), similar to our previous findings in GLUTag cells (Reimann *et al.* 2005), and suggesting the involvement of voltage gated Na$^+$ currents.

In whole cell recordings, with solutions designed to record Na$^+$ currents, large rapidly inactivating inward currents were detected, with a maximum peak amplitude of -131 ± 21 pA pF^{-1} at ~ 0 mV ($n = 15$, Fig. 1B and C). These were blocked by TTX, confirming their identity as V-gated Na$^+$ currents (Fig. 1F). Fitting a Boltzmann equation (eqn (1)) to the peak Na$^+$ current revealed half-maximal activation at -17.4 ± 1.0 mV. Inactivation, measured following conditioning prepulses to different voltages, was half-maximal at -46.1 ± 1.2 mV (Fig. 1D and E). In perforated patch recordings, action potentials

could still be evoked by current injection when Na$^+$ currents were blocked by TTX, but were wider, were elicited at a higher threshold and showed less of an overshoot (Fig. 1G and H). Spontaneous action potentials were reduced in frequency, but not abolished, by TTX (Fig. 1I).

The properties of the V-gated Na$^+$ current are typical of a number of members of the Scn family. To examine the potential identity of the underlying channel subunits, we interrogated microarray databases of FACS purified primary L-cells. The most highly expressed Scn α-subunits in L-cells were *scn3a*, $-5a$ and $-11a$ (Fig. 2A). These were further assessed by quantitative RT-PCR, confirming high expression of the TTX-sensitive Na$^+$ channel subunit *scn3a*, which was relatively specific for the L-cell population compared with non-L-cell neighbours (Fig. 2B). The finding that the TTX-resistant subunits *scn5a* and *scn11a* were expressed at 30- to 100-fold lower levels than *scn3a* explains why the Na$^+$ currents were sensitive, not resistant, to TTX. S*cn1a* was detected in GLUTag cells by microarray and previously by qRT-PCR (Reimann *et al.* 2005), but was not well represented in primary L-cells. By microarray, L-cells also expressed the β-subunits *scn1b* and $-3b$.

The functional importance of membrane depolarisation was examined by measuring GLP-1 secretion from primary colonic cultures. Basal GLP-1 secretion was inhibited $\sim 50\%$ by the K$_{ATP}$ channel opener, diazoxide (340 μmol l^{-1}, Fig. 3A), consistent with the previous identification of functional K$_{ATP}$ channels in primary L-cells (Reimann *et al.* 2008). In the continued presence of diazoxide, GLP-1 secretion was triggered dose dependently by KCl (Fig. 3A). These findings indicate that GLP-1 secretion is voltage dependent, likely to be mediated by the activation of V-gated Ca^{2+} channels. Given that GLP-1 secretion is 2-fold higher in the absence than the presence of diazoxide, this suggests that cultured L-cells have a basal secretory tone which can be overcome by increasing the potassium permeability. This is consistent with the finding that single identified L-cells fire action potentials from a resting relatively depolarised membrane potential of ~ -50 mV in perforated patch recordings (Fig. 1I) (Reimann *et al.* 2008).

The importance of voltage-gated Na$^+$ channels was examined both under basal conditions and in response to a glutamine nutrient stimulus. GLP-1 release was inhibited 13% ($n = 9$, $P < 0.01$) by TTX in the absence of added nutrient. Glutamine at 10 mmol l^{-1} stimulated a 1.95 ± 0.16 -fold increase in secretion which was also inhibited 21% by TTX ($n = 9$, $P < 0.01$, see Fig. 3B). This supports the idea that both basal and glutamine-triggered secretion are sustained by Na$^+$ channel-dependent electrical activity.

In electrophysiological recordings performed in the presence of TTX, we observed a residual inward current that inactivated more slowly than the TTX-sensitive Na$^+$
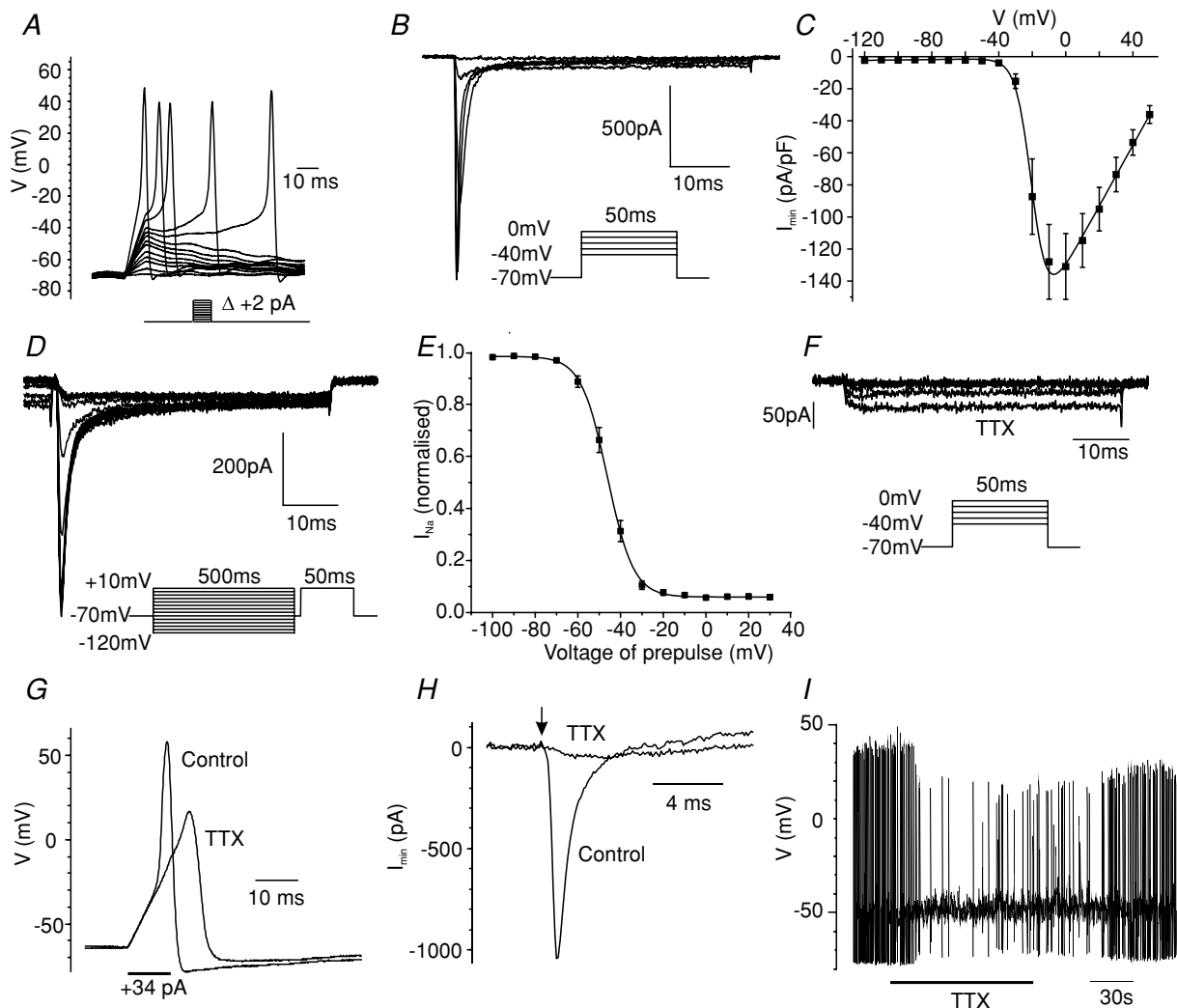
Figure 1. Na⁺-dependent electrical activity

A, perforated patch current clamp recording of an L-cell, showing action potentials triggered by depolarising current injections. Current was injected to maintain the cell at −70 mV, and a series of 10 ms current pulses were applied, increasing in magnitude by 2 pA. The pulse protocol is illustrated below. *B*, current responses to 50 ms voltage steps of 10 mV increments, applied at ∼1 Hz, from a holding potential of −70 mV, in a standard whole-cell voltage-clamp recording. The inset shows the voltage pulse protocol. *C*, current–voltage relationship of the peak currents obtained using the experimental set-up shown in *B* (*n* = 15). The line shows the best fit of the mean data using eqn (1), with the following parameters: g_{max} = 1.9 nS pF⁻¹, V_h, = −19 mV, k = 5 mV, V_{rev} = 69 mV. *D*, voltage dependence of the steady state inactivation in standard whole cell voltage clamp recordings was measured by holding the membrane potential for 500 ms at conditioning voltages from −120 to +10 mV (at 10 mV increments) before stepping to −70 mV for 1 ms and then +10 mV for 50 ms. The inset shows the voltage pulse protocol. Only the current response to the test pulse to +10 mV is shown. *E*, the peak currents obtained as in *D* (*n* = 10) were normalised to the maximum peak current, and plotted against the holding potential applied during the conditioning pulse. The line shows the best fit of the mean data to eqn (2): V_h = −46 mV; k = 6 mV. *F*, currents remaining in the presence of TTX (0.3 μmol l⁻¹), recorded as in *B*. *G*, perforated patch current clamp recording of an L-cell, showing action potentials evoked by the current injection protocol shown in *A*. Traces depict the response to injection of a +34 pA depolarising current for 10 ms, in either the absence or the presence of TTX (0.3 μmol l). *H*, voltage clamp recording of the cell shown in *G*, demonstrating that the inward Na⁺ current triggered by a voltage step from −70 mV to −10 mV (beginning at the arrow) was abolished by TTX (0.3 μmol l⁻¹). *I*, spontaneous action potentials in the cell depicted in *G* and *H* above. The cell was maintained in a depolarized state by continuous injection of a small (<2 pA) depolarising current. TTX (0.3 mol l⁻¹) was applied for the period represented by the horizontal bar.

current (Fig. 4A). Replacement of Na^+ with $NMDG^+$ in the extracellular solution had no effect on the properties of this current, indicating that it was not attributable to a TTX-insensitive Na^+ current (data not shown). It was, however, blocked by 5 mmol l^{-1} $CoCl_2$, and was also observed when Ca^{2+} was replaced by Ba^{2+}, properties characteristic of V-gated Ca^{2+} currents (Fig. 4B–E). When we examined the voltage dependence of the peak, rather than the steady state, Ca^{2+} current, we observed a clear shoulder to the current at relatively hyperpolarised potentials, suggesting the presence of both low and high voltage activated channels (Fig. 4C). Indeed the data were well fitted with a two-component Boltzmann curve (eqn (4)), revealing that $17 \pm 2\%$ of the current was half-maximally activated at -40 ± 1 mV, and $83 \pm 2\%$ at -5 ± 1 mV ($n = 16$). Approximately half the Ca^{2+} current was inactivated by prepulses to more depolarised potentials, (Fig. 4F).

The molecular identity of channel subunits underlying the Ca^{2+} current was investigated by examining which Ca^{2+} channel α-subunits (*cacna1*) were expressed in

L-cells, as determined by microarray analysis. As shown in Fig. 5A, expression levels of P/Q-type, L-type and T-type subunits in L-cells were above the cut-off of 100, which we have found to represent levels of expression reliably reconfirmed by RT-PCR. These findings were verified by quantitative RT-PCR (Fig. 5B). Compared with GLUTag cells, however, L-cells had considerably lower expression of both L-type and N-type subunits. The T-type channels are likely to correspond to the component of the Ca^{2+} current activated at more hyperpolarised potentials.

We examined the functional importance of different Ca^{2+} channel types on basal and glutamine-stimulated GLP-1 secretion from primary cultures. Under basal conditions, secretion was inhibited $16 \pm 4\%$ by the L-type Ca^{2+} channel blocker nifedipine (10 μmol l^{-1}, $n = 9$, $P = 0.007$) and $28 \pm 6\%$ by ω-conotoxin MVIIC (1 μmol l^{-1}, $n = 6$, $P = 0.007$), an inhibitor of Q-type Ca^{2+} channels, but was not blocked by agatoxin-IVA (data not shown). As agatoxin has a greater specificity for P-type channels, and ω-conotoxin MVIIC for Q-type channels, our data suggest a greater importance for the Q-type
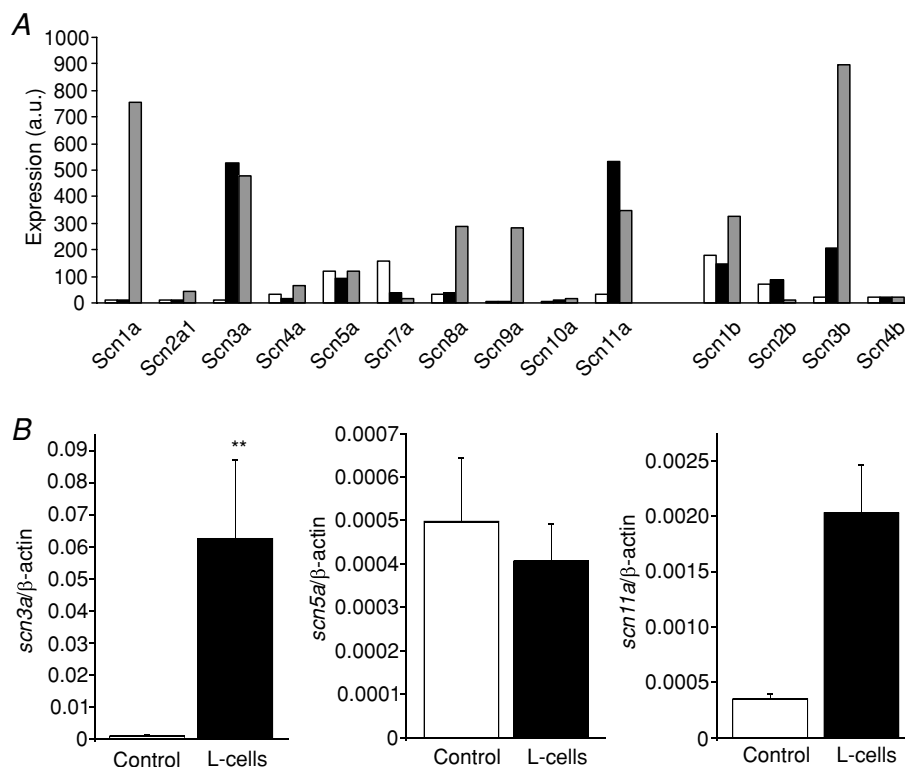

Figure 2. Na^+ channel subunit expression
A, expression of different Scn α- and β-subunit mRNAs in colonic L-cells (black bars), control colonic cells (open bars) and GLUTag cells (grey bars), assessed by Affymetrix microarray. Expression was evaluated by RMA analysis, and is depicted on an arbitrary scale on which values >100 represent expression that can be reliably detected by quantitative RT-PCR ($n = 2$–3 per cell type). B, expression of *scn3a*, *scn5a* and *scn11a* were confirmed by quantitative RT-PCR, and depicted relative to the expression of β-actin in the same sample: L-cells (black bars, $n = 3$), control colonic cells (open bars, $n = 3$). **Significant difference between L-cells and controls at a level of $P < 0.01$ (by Student's *t* test performed on ΔC_T data).

currents. The same pattern was observed in the presence of 10 mmol l^{-1} glutamine (see Fig. 5C). The T-type Ca^{2+} channel blocker NNC 55-3096 did not inhibit secretion (data not shown), perhaps reflecting the known off-target effects of T-type inhibitors (Huc *et al.* 2009), and was not therefore investigated further. No inhibition was observed with the N-type blocker, ω-conotoxin GVIA ($1 \text{ } \mu\text{mol l}^{-1}$), consistent with the lack of N-type Ca^{2+} channel subunits by expression analysis.

As L-type and P/Q-type Ca^{2+} channels are typically activated by more depolarised membrane potentials, we also examined the effect of the inhibitors on GLP-1 secretion triggered by 70 mmol l^{-1} KCl plus diazoxide. Under these conditions, release was blocked 23% by nifedipine and 39% by ω-conotoxin MVIIC (Fig. 5D). TTX was ineffective as expected (data not shown), as the depolarising conditions would be predicted to inactivate V-gated Na^+ channels and abolish action potential firing.

We examined the expression and properties of V-gated K^+ channels which typically underlie the down-stroke of the action potential and the after-hyperpolarisation. The majority ($89 \pm 2\%$, $n = 8$) of the voltage-dependent K^+ current was TEA sensitive (Fig. 6A–C), and of the $\sim$10% remaining in TEA, $51 \pm 8\%$ was blocked by addition of 10 mmol l^{-1} 4-AP (data not shown). By microarray analysis, we detected expression of a range of subunits reported to function as voltage gated K^+ channels (Fig. 6D) (Harmar *et al.* 2009). Interestingly, the most highly expressed K^+ channel gene-family member in L-cells was *kcnq1*, a channel that requires a KCNE binding partner, in this case likely to be *kcne3* (Fig. 6D inset). As human poly-morphisms in *kcnq1* are associated with reduced incretin levels (Mussig *et al.* 2009), we reconfirmed expression of *kcnq1/kcne3* by RT-PCR (Fig. 6F) and tested for a KCNQ1/KCNE3 current using the inhibitor chromanol 293B ($10 \text{ } \mu\text{mol l}^{-1}$). KCNQ1/KCNE3 currents are reportedly voltage insensitive (Schroeder *et al.* 2000), and were therefore evaluated following subtraction of the V-sensitive K^+ current component. Only a very small chromanol sensitive current was observed (Fig. 6E), which reversed at $\sim$−40 mV, less negative than predicted for a K^+ current. We suspect this is a combination of a chromanol sensitive K^+ current and a time-dependently decreasing leak conductance.

Discussion

This study establishes the importance of Na^+-dependent action potentials and voltage gated L- and Q-type Ca^{2+} currents for the control of basal and stimulated GLP-1 secretion. It suggests that modulation of the firing frequency of L-cells is one mechanism by which nutrients, such as glutamine, may trigger GLP-1 release.

The finding that primary L-cells fire action potentials is interesting, as the few other primary enteroendocrine cells that have been studied to date, such as ECL cells, have been considered to be electrically unexcitable (Prinz *et al.* 2003). Although one report described a TTX-sensitive current of small amplitude in ECL cells, it failed to demonstrate an effect of TTX on hormone secretion (Lindstrom *et al.* 2001). By contrast, ECL cells undisputedly express voltage-gated Ca^{2+}-channels (Bufler *et al.* 1998; Lindstrom *et al.* 2001) that regulate hormone secretion (Lindstrom *et al.* 2001; Bjorkqvist *et al.* 2005), yet no action potentials have been reported to date. The difference between L-cells and ECL cells may reflect their differing functions
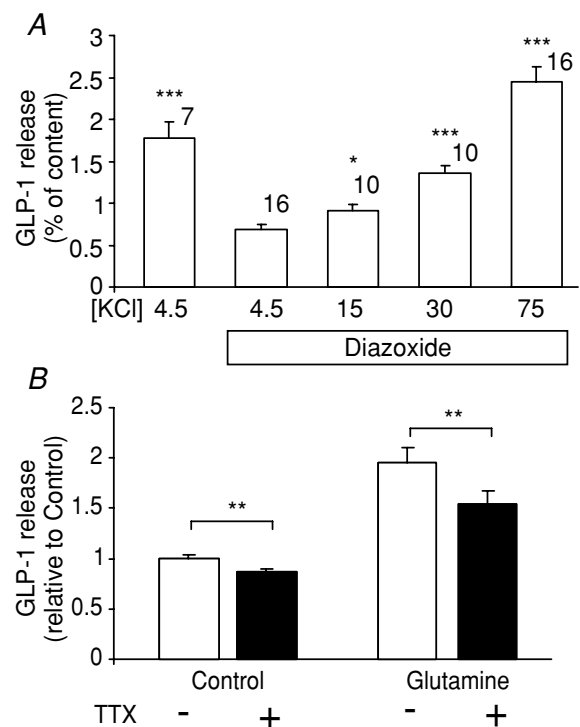

Figure 3. Voltage-dependent GLP-1 release from primary colonic cultures

A, GLP-1 release was measured from primary colonic cultures incubated for 2 h in the presence of different KCl concentrations (in mmol l^{-1}) and diazoxide (340 μmol l^{-1}), as indicated. GLP-1 was measured in the supernatant and cell lysate, and is expressed relative to the total content in each well. The numbers of wells are indicated above the bars. Significance was tested by Student's *t* test, and is shown relative to secretion in the presence of 4.5 mmol l^{-1} KCl plus diazoxide; *$P < 0.05$, ***$P < 0.001$. *B*, GLP-1 release from primary cultures incubated for 2 h in the presence of TTX (0.3 μmol l^{-1}) and/or glutamine (10 mmol l^{-1}), as indicated ($n = 9$ each). Secretion was measured as in *A*, and is expressed relative to the secretory rate measured in control wells of the same experiment. The significance of the effect of TTX was assessed by single sample *t* test under basal conditions, and by regression analysis in the presence of glutamine, with the experiment as an independent dummy variable to compensate for different effectiveness of glutamine between experimental days: **$P < 0.01$.

and morphology. It is possible, however, that electrical activity is a more general characteristic of primary enteroendocrine cells, but that the ability to detect it is dependent on the experimental preparation. In support of this idea, we rarely observed electrical activity in acutely dissociated L-cells, and it was only with the development of protocols that supported L-cell survival for over a week in a mixed cell culture that we became able to record reproducible action potentials and large V-gated Na^+ currents. The observation that epithelial dissociation into single cells did not support subsequent L-cell survival and function may reflect an importance of maintaining contacts with neighbouring cells, but might also relate to the use of collagenase for tissue dispersal. The cultures used for electrophysiology and secretion analysis, however, were derived from larger cell clusters, in which individual

L-cells would have been at least partially protected from extensive collagenase damage. The electrical activity of primary L-cells is similar to our previous observations that the GLP-1 secreting cell line, GLUTag, also fires Na^+ channel-dependent action potentials (Reimann & Gribble, 2002).

When we worked with GLUTag cells, we observed nutrient triggered action potentials but could not establish a functional link between electrical activity and secretion, as TTX did not inhibit glucose-triggered GLP-1 release (Reimann *et al.* 2005). The present study shows, however, that secretion from cultured primary L-cells is TTX sensitive both under basal conditions and during stimulation with glutamine, indicating that GLP-1 release from primary L-cells is dependent on electrical activity. The effect of TTX on basal secretion suggests that L-cells
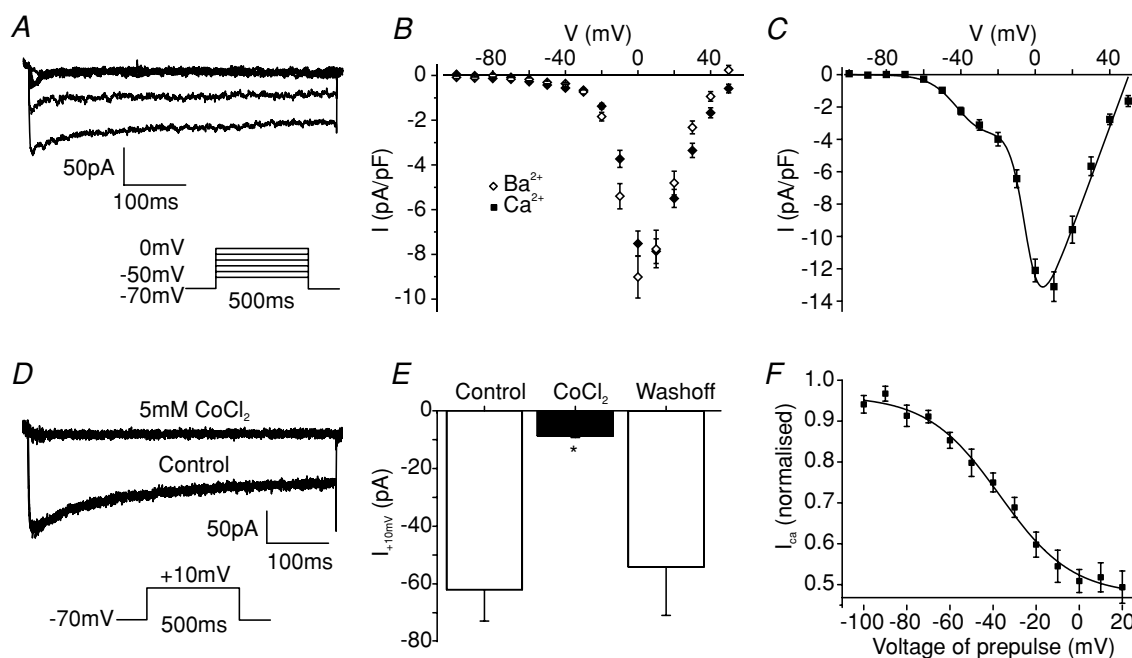

Figure 4. Voltage gated Ca^{2+} currents
A, current responses to 500 ms voltage steps of 10 mV increments from a holding potential of -70 mV, in a standard whole-cell voltage-clamp recording applied at $\sim$1 Hz. The inset shows the voltage pulse protocol. TTX at 0.3 μmol l^{-1} was included to block Na^+ currents. *B*, current–voltage relationship of the steady state currents obtained using the experimental set-up shown in *A* (filled diamonds, $n = 16$). Similar currents were recorded when extracellular Ca^{2+} was replaced by Ba^{2+} as the charge carrier (open diamonds, $n = 11$). *C*, current–voltage relationship of the peak currents obtained as in *A* ($n = 16$). The curve shows the best fit of the mean data to eqn (4), with the parameters: $g_{max1} = 265$ pS pF^{-1}, $V_{h1} = -4.7$ mV, $k_1 = 4$ mV, $g_{max2} = 50$ pS pF^{-1}, $V_{h2} = -40$ mV, $k_2 = 8$ mV, $V_{rev} = 50$ mV. *D*, current responses to 500 ms voltage steps to -10 mV from a holding potential of -70 mV (voltage pulse protocol shown in the inset) in the presence 0.3 μmol l^{-1} TTX, and 5 mmol l^{-1} Co^{2+} as indicated in standard whole cell voltage clamp recordings. *E*, mean steady state current before, during and after addition of 5 μmol l^{-1} $CoCl_2$ ($n = 4$), recorded as in *D*. Error bars represent 1 s.e.m. and significance was tested comparing the current during application of the inhibitor with the current before inhibitor addition using a paired *t* test. **$P < 0.01$. *F*, voltage-dependent Ca^{2+} channel inactivation was determined by measuring the peak current response to a 200 ms test pulse to 0 mV, after 500 ms prepulses to different potentials in standard whole cell voltage clamp recordings. Currents were normalised to the maximum peak current, and plotted against the holding potential applied during the conditioning pulse. The data were fitted with eqn (2): $V_h = -37$ mV, $k = 17$ mV, $A = 0.5$.
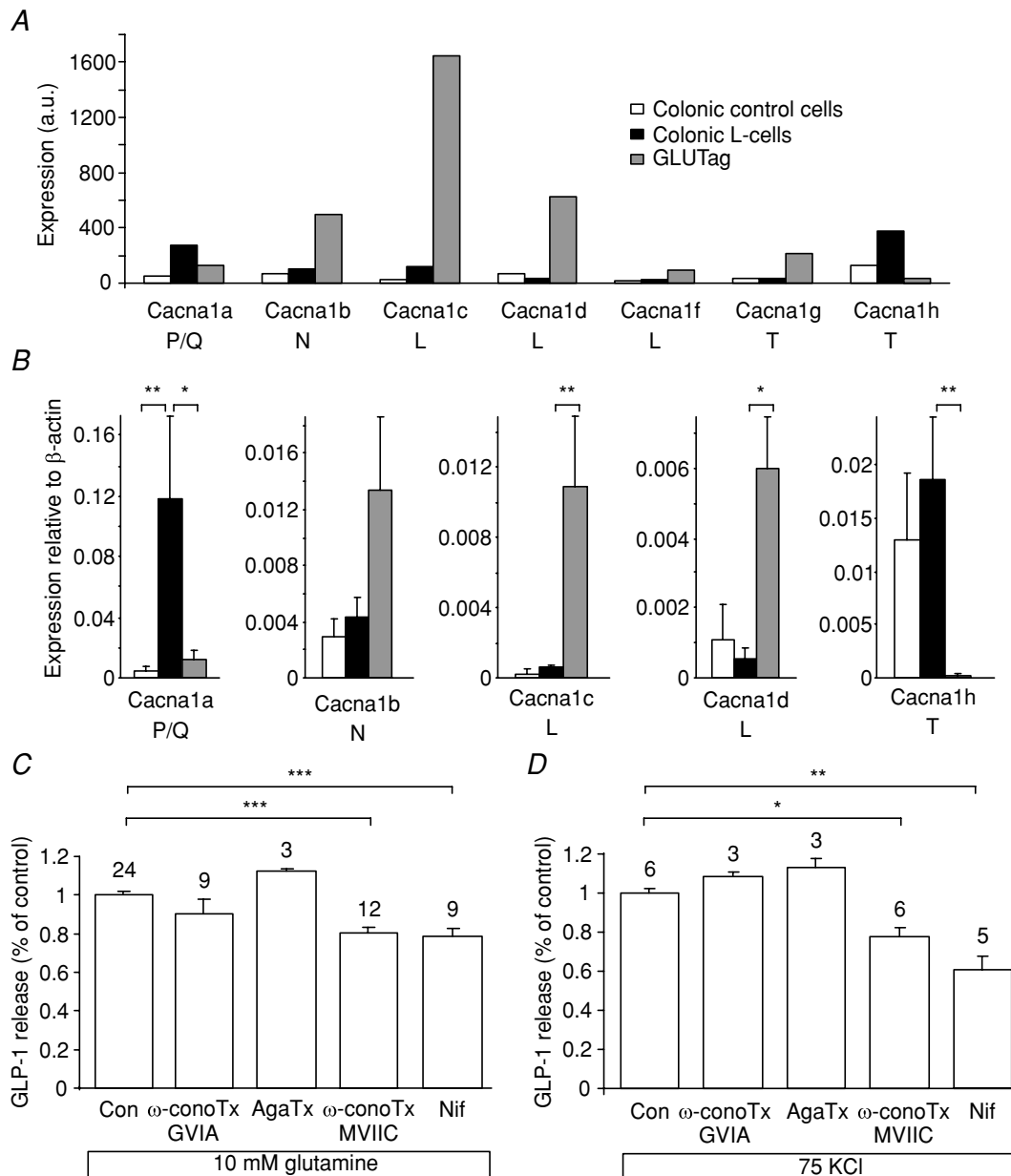
Figure 5. Expression and function of Ca²⁺ channel subtypes

A, expression of different *cacn* α-subunit mRNAs in colonic L-cells (black bars) control colonic cells (open bars) and GLUTag cells (grey bars), assessed by Affymetrix microarray. Expression was evaluated by RMA analysis, and is depicted on an arbitrary scale on which values >100 represent expression that can be reliably detected by quantitative RT-PCR ($n = 2$–3 per cell type). *B*, expression of the most highly expressed *cacna1* subunits (as found in *A*) was confirmed by quantitative RT-PCR, and depicted relative to the expression of *β-actin* in the same sample: L-cells (black bars, $n = 3$), control colonic cells (open bars, $n = 3$), GLUTag cells (grey bars, $n = 3$). * and ** represent a significant difference between control-cells and GLUTag cells compared to L-cells at a level of $P < 0.05$ and $P < 0.01$, respectively (by Student's *t* test performed on ΔC_T data). *C* and *D*, GLP-1 release was measured from primary colonic cultures incubated for 2 h in the presence of 10 mmol l⁻¹ glutamine (*B*) or 75 mmol l⁻¹ KCl plus 340 μmol l⁻¹ diazoxide (*C*), plus the inhibitors indicated. No inhibitor control (Con), ω-conotoxin GVIA (ω-conoTx GVIA, 1 μmol l⁻¹), agatoxin IVA (AgaTx, 0.2 μmol l⁻¹), ω-conotoxin MVIIC (ω-conoTx MVIIC, 1 μmol l⁻¹), nifedipine (Nif, 10 μmol l⁻¹). GLP-1 in the supernatant was measured as a percentage of the total GLP-1 content in each well, and is expressed relative to the secretion triggered by glutamine or 75 mmol l⁻¹ KCl in the absence of inhibitor. Numbers of wells are indicated above the bars. Significance was tested by Student's *t* test; *$P < 0.05$, **$P < 0.01$, ***$P < 0.001$.

are partially depolarised and electrically active even in the absence of added nutrient, consistent with the finding that secretion was also reduced ~50% by diazoxide, which is predicted to hyperpolarise the L-cell membrane, as shown previously using GLUTag cells (Reimann & Gribble, 2002). This TTX sensitive component of basal secretion presumably reflects the ~50% of the Na^+ current that would not be subject to inactivation at the resting membrane potential of ~-50 mV. The ability of TTX to reduce glutamine triggered GLP-1 release indicates that action potential firing is also important for sustained nutrient-dependent secretion. However, under both basal and stimulated conditions, it is noteworthy that the inhibitory effect of TTX on secretion was only partial, perhaps reflecting the finding that action potentials could still be triggered in the presence of TTX, albeit with
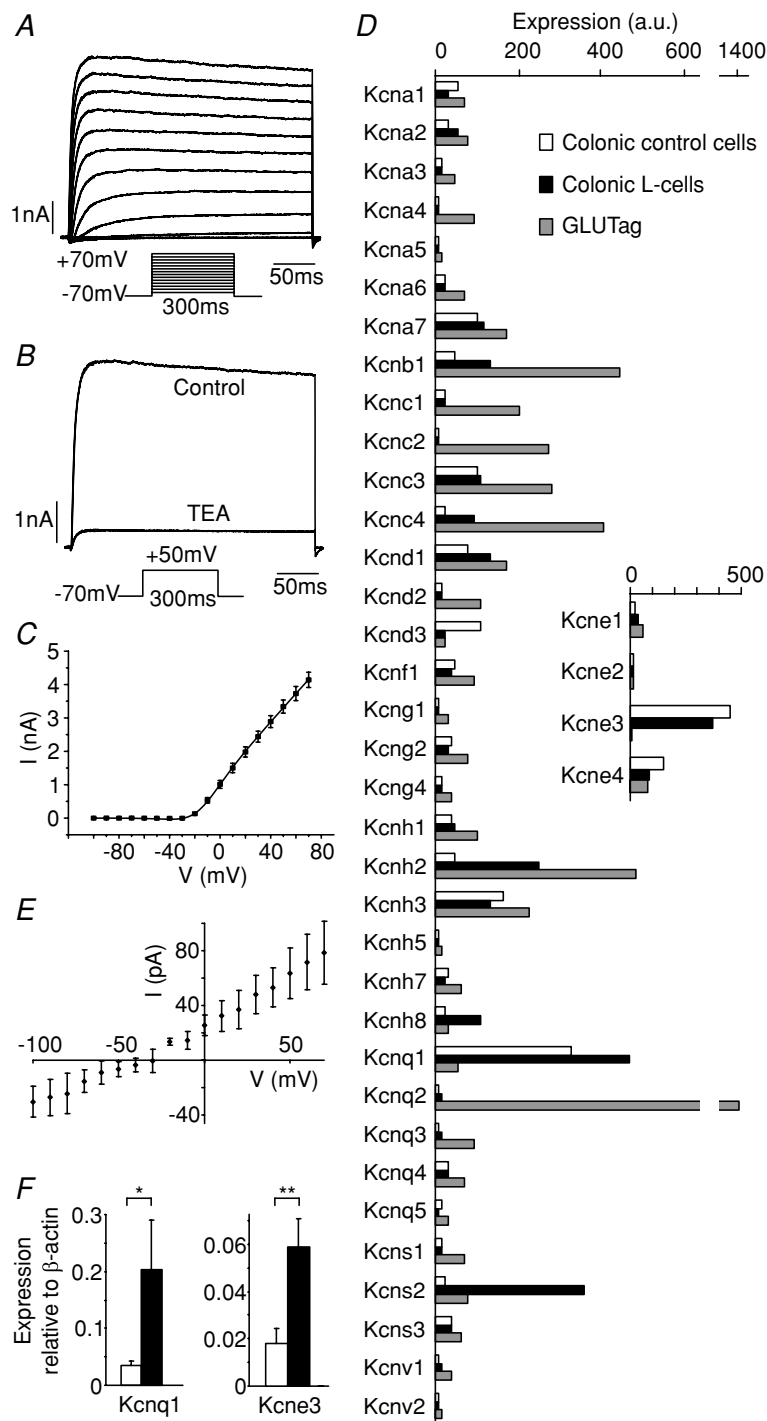

Figure 6. Voltage gated K^+ currents
A, current responses to 300 ms voltage steps of 10 mV increments from a holding potential of −70 mV, in a standard whole-cell voltage-clamp recording applied at ~1 Hz in the presence of 0.3 μmol l^{-1} TTX. The inset shows the voltage pulse protocol. *B*, current responses to a test pulse to +50 mV in the absence and presence of TEA (10 mmol l^{-1}), recorded as in *A*. *C*, current–voltage relationship of the steady state currents, recorded as in *A*. The line shows the best fit of the mean data with eqn (3): $g_{max} = 27$ nS, $V_h = 5.2$ mV, $k = 15$ mV, $n = 16$. *D*, expression of subunits encoding voltage gated K^+ channels in colonic L-cells (black bars), control colonic cells (open bars) and GLUTag cells (grey bars), assessed by Affymetrix microarray. Expression was evaluated by RMA analysis, and is depicted on an arbitrary scale on which values >100 represent expression that can be reliably detected by quantitative RT-PCR ($n = 2$–3 per cell type). Inset shows expression of *kcne* subunits, which act as partners to KCNQ1. *E*, steady state currents were recorded as in *A* in the absence and presence of chromanol 293B (10 μmol l^{-1}). V-dependent currents (measured using leak subtraction software) were subtracted from the total currents to obtain the V-independent current component. The figure shows the chromanol sensitive V-independent current, obtained by subtracting the V-independent current in the absence of chromanol from that in the presence of the drug ($n = 5$). *F*, expression of *kcnq1 and kcne3* was confirmed by quantitative RT-PCR, and depicted relative to the expression of *β-actin* in the same sample: L-cells (black bars, $n = 3$), control colonic cells (open bars, $n = 3$). * and ** represent a significant difference between control cells and L-cells at a level of $P < 0.05$ and $P < 0.01$, respectively (by Student's *t* test performed on ΔC_T data).

a higher threshold and lower frequency. In L-cells *in situ*, where stimulus detection may be restricted to either the apical or the basolateral membrane, the relationship between Na^+-dependent action potentials and GLP-1 secretion may also differ from that measured in our non-polarised primary cultures.

The finding of cobalt-sensitive Ca^{2+} currents in L-cells is not surprising, as voltage-dependent Ca^{2+} channels underlie activity-triggered secretion in a range of endocrine and neuronal cell types. Microarray analysis suggested that these might be attributable to T-, L- and/or P/Q-type channels. T-type Ca^{2+} channels are typically activated at low (relatively hyperpolarised) membrane potentials, and are therefore likely to underlie the first peak of Ca^{2+} currents detected at membrane potentials positive to ∼−50 mV. The functional importance of the T-type component is difficult to evaluate pharmacologically, as there is a lack of inhibitors specific for T-type Ca^{2+} channels (Huc *et al.* 2009). In other cell types, however, T-type Ca^{2+} channels modulate membrane excitability, as they are activated by small changes in the membrane potential, and in neurosecretory chromaffin cells they have been linked to the stimulation of fast exocytosis (Giancippoli *et al.* 2006). L- and P/Q-type channels, by contrast, are high voltage activated channels, requiring depolarisations to more positive membrane potentials for activation. Inhibitors of L-type and Q-type Ca^{2+} channels reduced GLP-1 secretion under basal conditions and in response to stimulation by glutamine or KCl. The inhibition of basal secretion suggests that background electrical activity is sufficient to activate these classes of Ca^{2+} channel.

Although the Na^+ and Ca^{2+} currents in primary L-cells are electrophysiologically similar to those reported in GLUTag cells, their subunit composition appears to be different. We reported previously, and show here by microarray, that the predominant Na^+ channel α-subunit in GLUTag cells is s*cn1a* (Reimann *et al.* 2005). In primary cells, by contrast, we find that the Na^+ current is almost certainly attributable to s*cn3a*. The voltage gated Ca^{2+} current in GLUTag cells was previously attributed to L- and N-type Ca^{2+} channels, as also shown here by microarray and qRT-PCR, which found high expression in GLUTag cells of *cacna1b* (Ca_v2.2, N-type), *cacna1c* (Ca_v1.2, L-type) and *cacna1d* (Ca_v1.3, L-type). Consistent with the low expression of *cacna1b* in primary L-cells, however, we did not observe an inhibitory effect of the N-type blocker ω-conotoxin GVIA on GLP-1 secretion from primary cultures. In terms of its Na^+ and Ca^{2+} currents, GLUTag cells are not, therefore, an accurate model of the primary colonic L-cell.

The major part of of the voltage-dependent K^+ current in L-cells was TEA sensitive and non-inactivating. Whilst we identified a number of K^+ channel subunits by microarray analysis that might underlie this current, we did not

attempt to distinguish them further pharmacologically. Expression analysis revealed that one of the most highly expressed K^+ channel subunits in L-cells is *kcnq1*, which is likely to form currents together with the most highly expressed KCNE subunit, KCNE3 (Preston *et al.* 2010). KCNQ1 and KCNE3 have been localised immunohistochemically to the basolateral membrane surface of cells in colonic crypts (Preston *et al.* 2010). They form a voltage-insensitive basolateral K^+ current that is believed to act as a counter-current responsible for maintaining apical cAMP-stimulated Cl^- fluxes, and may also maintain charge balance when glucose is transported with Na^+ by apically located SGLT in the kidney (Vallon *et al.* 2005). The chromanol sensitive K^+ current we observed in L-cells was not large, perhaps because KCNQ1/KCNE3 currents are found in crypts rather than villi (Preston *et al.* 2010). The role of KCNQ1 in L-cells therefore remains unclear, and it is possible that the diabetes-associated human polymorphisms in *kcnq1* (Mussig *et al.* 2009) may influence incretin levels indirectly by altering crypt function or L-cell number, rather than through direct modulation of mature L-cells.

Conclusions and physiological relevance

It seemed paradoxical, when we were studying GLUTag cells, that we observed Na^+ channel-dependent electrical activity, but no effect of TTX on GLP-1 release (Reimann *et al.* 2005). In primary L-cells, however, we found that electrical activity was coupled to secretion under basal and glutamine-stimulated conditions. Nevertheless, the precise role of Na^+-dependent action potentials remains uncertain. Pancreatic β-cells are electrically active, but their action potentials are carried by Ca^{2+} rather than Na^+ ions (Rorsman, 1997), providing a direct link between activity and secretion. Ca^{2+} currents are similarly likely to underlie the continued, albeit altered, electrical activity of primary L-cells in the presence of TTX. Na^+-dependent action potentials are better recognised for their roles in nerve and muscle, where they convert small localised signals, e.g. from synaptic activity, to a frequency-encoded message that can travel large distances. As L-cells have processes, sometimes quite thin, extending to the gut lumen (Eissele *et al.* 1992; Parker *et al.* 2010), as well as basolateral extensions (Karaki *et al.* 2006), it is tempting to speculate that they also use action potentials to transmit messages from one part of the cell to another. Currents generated by glucose uptake on SGLT1, for example, are small and probably localised to the apical membrane, so would be a prime candidate to benefit from action potential generation as a mechanism to carry the signal to the basal pole of L-cells where the secretory vesicles reside. Overall, our data clearly paint a picture of an electrically excitable L-cell using action potentials to encode and relay

signals that directly modulate GLP-1 secretion. Under-standing how other second messenger systems interlink with this signalling pathway is likely to be central to developing L-cell targeted therapeutics that could be used for the treatment of diabetes and obesity.

References

Bjorkqvist M, Bernsand M, Eliasson L, Hakanson R & Lindstrom E (2005). Somatostatin, misoprostol and galanin inhibit gastrin- and PACAP-stimulated secretion of histamine and pancreastatin from ECL cells by blocking specific Ca^{2+} channels. *Regulatory Peptides* **130**, 81–90.

Bufler J, Choi GC, Franke C, Schepp W & Prinz C (1998). Voltage-gated Ca^{2+} currents in rat gastric enterochromaffin-like cells. *Am J Physiol Cell Physiol* **274**, C424–C429.

Drucker DJ, Jin TR, Asa SL, Young TA & Brubaker PL (1994). Activation of proglucagon gene-transcription by protein kinase-A in a novel mouse enteroendocrine cell-line. *Mol Endocrinol* **8**, 1646–1655.

Drucker DJ & Nauck MA (2006). The incretin system: glucagon-like peptide-1 receptor agonists and dipeptidyl peptidase-4 inhibitors in type 2 diabetes. *Lancet* **368**, 1696–1705.

Eissele R, Goke R, Willemer S, Harthus HP, Vermeer H, Arnold R & Goke B (1992). Glucagon-like peptide-1 cells in the gastrointestinal-tract and pancreas of rat, pig and man. *Eur J Clin Invest* **22**, 283–291.

Elliott RM, Morgan LM, Tredger JA, Deacon S, Wright J & Marks V (1993). Glucagon-like peptide-1(7–36)amide and glucose-dependent insulinotropic polypeptide secretion in response to nutrient ingestion in man – acute postprandial and 24-h secretion patterns. *J Endocrinol* **138**, 159–166.

Giancippoli A, Novara M, de Luca A, Baldelli P, Marcantoni A, Carbone E & Carabelli V (2006). Low-threshold exocytosis induced by cAMP-recruited $Ca_V 3.2$ (α_{1H}) channels in rat chromaffin cells. *Biophys J* **90**, 1830–1841.

Gribble FM (2008). RD Lawrence Lecture 2008 – Targeting GLP-1 release as a potential strategy for the therapy of Type 2 diabetes. *Diabetic Med* **25**, 889–894.

Gribble FM, Williams L, Simpson AK & Reimann F (2003). A novel glucose-sensing mechanism contributing to glucagon-like peptide-1 secretion from the GLUTag cell line. *Diabetes* **52**, 1147–1154.

Harmar AJ, Hills RA, Rosser EM, Jones M, Buneman OP, Dunbar DR, Greenhill SD, Hale VA, Sharman JL, Bonner TI, Catterall WA, Davenport AP, Delagrange P, Dollery CT, Foord SM, Gutman GA, Laudet V, Neubig RR, Ohlstein EH, Olsen RW, Peters J, Pin JP, Ruffolo RR, Searls DB, Wright MW & Spedding M (2009). IUPHAR-DB: the IUPHAR database of G protein-coupled receptors and ion channels. *Nucleic Acids Res* **37**, D680–D685.

Herrmann C, Goke R, Richter G, Fehmann HC, Arnold R & Goke B (1995). Glucagon-like peptide-1 and glucose dependent insulin-releasing polypeptide plasma-levels in response to nutrients. *Digestion* **56**, 117–126.

Holst JJ (2007). The physiology of glucagon-like peptide 1. *Physiol Rev* **87**, 1409–1439.

Huc S, Monteil A, Bidaud I, Barbara G, Chemin J & Lory P (2009). Regulation of T-type calcium channels: Signalling pathways and functional implications. *Biochim Biophys Acta* **1793**, 947–952.

Karaki S, Mitsui R, Hayashi H, Kato I, Sugiya H, Iwanaga T, Furness JB & Kuwahara A (2006). Short-chain fatty acid receptor, GPR43, is expressed by enteroendocrine cells and mucosal mast cells in rat intestine. *Cell Tissue Res* **324**, 353–360.

Lindstrom E, Eliasson L, Bjorkqvist M & Hakanson R (2001). Gastrin and the neuropeptide PACAP evoke secretion from rat stomach histamine-containing (ECL) cells by stimulating influx of Ca^{2+} through different Ca^{2+} channels. *J Physiol* **535**, 663–677.

Mussig K, Staiger H, Machicao F, Kirchhoff K, Guthoff M, Schafer SA, Kantartzis K, Silbernagel G, Stefan N, Holst JJ, Gallwitz B, Haring HU & Fritsche A (2009). Association of type 2 diabetes candidate polymorphisms in KCNQ1 with incretin and insulin secretion. *Diabetes* **58**, 1715–1720.

Parker HE, Reimann F & Gribble FM (2010). Molecular mechanisms underlying nutrient-stimulated incretin secretion. *Expert Rev Mol Med* **12**, e1.

Preston P, Wartosch L, Gunzel D, Fromm M, Kongsuphol P, Ousingsawat J, Kunzelmann K, Barhanin J, Warth R & Jentsch TJ (2010). Disruption of the K^+ channel β-subunit KCNE3 reveals an important role in intestinal and tracheal Cl^{--} transport. *J Biol Chem* **285**, 7165–7175.

Prinz C, Zanner R & Gratzl M (2003). Physiology of gastric enterochromaffin-like cells. *Annu Rev Physiol* **65**, 371–382.

Reimann F & Gribble FM (2002). Glucose-sensing in glucagon-like peptide-1-secreting cells. *Diabetes* **51**, 2757–2763.

Reimann F, Habib AM, Tolhurst G, Parker HE, Rogers GJ & Gribble FM (2008). Glucose sensing in L cells: a primary cell study. *Cell Metab* **8**, 532–539.

Reimann F, Maziarz A, Flock G, Habib AM, Drucker DJ & Gribble FM (2005). Characterization and functional role of voltage gated cation conductances in the glucagon-like peptide-1 secreting GLUTag cell line. *J Physiol* **563**, 161–175.

Reimann F, Williams L, Xavier GD, Rutter GA & Gribble FM (2004). Glutamine potently stimulates glucagon-like peptide-1 secretion from GLUTag cells. *Diabetologia* **47**, 1592–1601.

Rorsman P (1997). The pancreatic β-cell as a fuel sensor: An electrophysiologist's viewpoint. *Diabetologia* **40**, 487–495.

Schroeder BC, Waldegger S, Fehr S, Bleich M, Warth R, Greger R & Jentsch TJ (2000). A constitutively open potassium channel formed by KCNQ1 and KCNE3. *Nature* **403**, 196–199.

Vallon V, Grahammer F, Volkl H, Sandu CD, Richter K, Rexhepaj R, Gerlach U, Rong Q, Pfeifer K & Lang F (2005). KCNQ1-dependent transport in renal and gastrointestinal epithelia. *Proc Natl Acad Sci U S A* **102**, 17864–17869.

Author contributions

All authors contributed to the design, analysis and interpretation of the data. F.M.G. and F.R. conceived the study and drafted the manuscript. The experiments

were performed in the Cambridge Institute for Medical Research.